Available online at www.sciencedirect.com

ScienceDirect

Scripta Materialia 105 (2015) 10–13

Scripta MATERIALIA

www.elsevier.com/locate/scriptamat

Stress relaxation in icosahedral small particles via generation of circular prismatic dislocation loops

M.Yu. Gutkin,[a,b,c,*] A.L. Kolesnikova,[a,c,d] S.A. Krasnitckii,[b,c] L.M. Dorogin,[c,d,e] V.S. Serebryakova,[c] A.A. Vikarchuk[d] and A.E. Romanov[c,d,f]

[a]*Institute of Problems of Mechanical Engineering, Russian Academy of Sciences, Bolshoj 61, Vasil. Ostrov, St. Petersburg 199178, Russia*

[b]*Department of Mechanics and Control Processes, Peter the Great St. Petersburg Polytechnic University, Polytekhnicheskaya 29, St. Petersburg 195251, Russia*

[c]*ITMO University, Kronverkskiy pr. 49, St. Petersburg 197101, Russia*

[d]*Togliatti State University, Belorusskaya 14, Togliatti 445667, Russia*

[e]*Institute of Physics, University of Tartu, Ravila 14c, Tartu 50411, Estonia*

[f]*Ioffe Physical Technical Institute, Russian Academy of Sciences, Polytekhnicheskaya 26, St. Petersburg 194021, Russia*

Received 25 March 2015; accepted 19 April 2015
Available online 29 April 2015

A theoretical model is developed that describes stress relaxation in icosahedral small particles through generation of circular prismatic dislocation loops. It is shown that loop generation is energetically favorable in the equatorial section of the particle, the radius of which is larger than the critical one. The dislocation loop then extends until it reaches its optimal radius which increases with particle size. Both the critical particle radius and optimal loop radius strongly depend on dislocation core energy.

Keywords: Icosahedral small particles; Residual stresses; Stress relaxation; Dislocation nucleation; Disclinations

Small particles made of materials with a face-centered cubic (fcc) crystalline structure often take the form of a polyhedron or prism having fivefold symmetry axes. Such objects are commonly called 'fivefold twinned' or, simpler, 'pentagonal' particles or rods. These nature artefacts were studied intensively over the last fifty years, but still demonstrate new and unusual properties [1–6]. It was also shown that the fraction of pentagonal particles in observed ensembles of nanoparticles of fcc metals and semiconductors can be large, see, for example, special studies [3] on gold nanoparticles.

It is well known that pentagonal rods and particles are subjected to residual mechanical stresses and store strain energy which is proportional to the particle volume. Nowadays there exists a number of models that explain the formation process and the physical properties of pentagonal small particles [1,7–11]. The models based on the disclination approach [7–9] seem to be the most natural and convenient ones for the quantitative description of the crystal lattice distortions in the pentagonal particles. The residual stresses and the strain energy can relax in the pentagonal particles through different mechanisms involving the generation of various crystal lattice defects such as dislocations, disclinations, low-angle grain boundaries and microtwins, the formation of open gaps, lattice mismatched layers and inclusions, surface whiskers, *etc.* [6,9,12–24]. Some of these mechanisms first predicted theoretically (see, for example, Refs. [12,13,15]), later received experimental confirmations. The reason for the manifestation of the variety of stress relaxation modes in pentagonal small particles still remains unexplained. Perhaps some relaxation processes develop consecutively with increasing the particle size, while others occur simultaneously.

What is evident, the onset of stress relaxation in pentagonal particles occurs through the generation of single defects such as a dislocation segment or an individual circular prismatic dislocation loop (CPDL). The conditions for CPDL generation in a pentagonal rod were studied for the first time in Ref. [25]. For equiaxial pentagonal particles, this problem has not been posed until now due to lack of suitable solutions for strain energy of a CPDL in an elastic sphere. Recently, such a solution has been delivered [26]

* Corresponding author at: Institute of Problems of Mechanical Engineering, Russian Academy of Sciences, Bolshoj 61, Vasil. Ostrov, St. Petersburg 199178, Russia.; e-mail addresses: m.y.gutkin@gmail.com; anna.kolesnikova.physics@gmail.com; krasnitsky@inbox.ru; dorogin@ut.ee; vlladllena@mail.ru; aer@mail.ioffe.ru

http://dx.doi.org/10.1016/j.scriptamat.2015.04.015
1359-6462/

and applied to the models of lattice mismatch relaxation via the generation of misfit CPDLs in bulk [27] and hollow [28] core–shell nanoparticles.

The present work is aimed at the analysis of the critical conditions for the generation of CPDLs in icosahedral small particles (ISPs) and at the finding of the optimal parameters for this process.

Consider an ISP in the initial state before stress relaxation. The geometric model of the ISP made of fcc material can be imaged as composed of 20 tetrahedra with {1 1 1}-type faces [8]. When these tetrahedra are glued together, it is required to have six positive wedge disclinations of strength $\omega \approx 2\pi - 10\sin^{-1}\left(\frac{1}{\sqrt{3}}\right) \approx 7°21' \approx 0.128$ to maintain ISP continuity. Wedge disclinations pass through the opposite vertices of the icosahedron [10]. For the sake of simplicity, one can replace the icosahedron with an elastic sphere containing either six discrete disclinations or a distributed stereo disclination which is also known as Marks–Yoffe disclination [8]. Then, the stress state of the ISP of radius a made of elastically isotropic materials is characterized by the following three non-vanishing stress tensor components [8]:

$$\sigma_{RR} = 2A\chi \ \ln(R/a), \quad \sigma_{\varphi\varphi} = \sigma_{\theta\theta} = \sigma_{RR} + A\chi, \tag{1}$$

where $A = \frac{2G(1+\nu)}{3(1-\nu)}$, $\chi = \frac{3\omega}{2\pi} \approx 0.0613$, G is the shear modulus and ν is the Poisson ratio. The hydrostatic stress component σ and the strain energy E_{ISP} of the ISP are given by:

$$\sigma = \frac{1}{3}(\sigma_{RR} + \sigma_{\phi\phi} + \sigma_{\theta\theta}) = 2A\chi \left[\ln\left(\frac{r}{a}\right) + \frac{1}{3}\right], \tag{2}$$

$$E_{\mathrm{ISP}} = \frac{4\pi}{9} A\chi^2 a^3. \tag{3}$$

From the latter formulas, important conclusions can be made. First, the strain energy grows rapidly with the ISP radius, $E_{\mathrm{ISP}} \sim a^3$, and, therefore relaxation processes become highly expected in growing ISPs. Second, the hydrostatic stress is negative in the central region of the ISP, if $R < a \ \exp(-1/3) \approx 0.72a$, and reaches the highest value in the center. Third, the hydrostatic stress is positive in the peripheral region of the ISP, if $R > 0.72a$, and on the surface ($R = a$) biaxial tension equals $2A\chi/3 \approx G/20$, for $\nu = 0.3$. Such high tensile stresses are expected to stimulate vacancy nucleation at the ISP surface and vacancy migration to ISP central region being under high hydrostatic compression. In real ISPs, the cores of six wedge disclinations can serve as the channels for enhanced vacancy pipe diffusion from the ISP surface to its center. Reaching the ISP center, the vacancies coagulate and form either a pore or a prismatic dislocation loop. It seems reasonable that at the beginning of the relaxation process, the vacancies first form the loop which then increases in size and, after reaching some limit radius, transforms into a pore.

In the present short paper, we consider only the first stage of the stress relaxation in ISPs through the formation of vacancy type CPDLs.

The change in the total energy of the system due to the generation of a CPDL is $\Delta E = E_{\mathrm{fin}} - E_{\mathrm{in}}$, where $E_{\mathrm{in}} = E_{\mathrm{ISP}}$ is the total energy of the ISP in the initial state (Fig. 1a) before relaxation that is the strain energy of the distributed stereo disclination, which is an intrinsic defect in the ISP, and $E_{\mathrm{fin}} = E_{\mathrm{ISP}} + E_{\mathrm{CPDL}} + E_{\mathrm{int}}$ is the total energy of the ISP in its final relaxed state (Fig. 1b). Here E_{CPDL} is the self-energy of the CPDL including both strain and core energy terms, and E_{int} is the energy of interaction between the CPDL and the distributed stereo disclination. Thus, the energy change is given by $\Delta E = E_{\mathrm{CPDL}} + E_{\mathrm{int}}$.

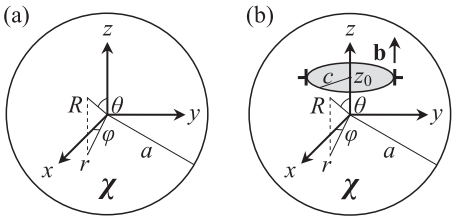

Figure 1. Schematics for the stress relaxation process in an ISP of radius a through generation of a CPDL of radius c with Burgers vector b placed coaxially at the distance z_0 from the ISP center: (a) the initial dislocation free state of the ISP, (b) the relaxed state of the ISP with a CPDL. The Cartesian (x, y, z), cylindrical (r, φ, z) and spherical (R, φ, θ) coordinates are shown.

The self-energy of the CPDL in an elastic sphere with free surface can be written as [26]:

$$E_{\mathrm{CPDL}} = {}^{\infty}E_{\mathrm{CPDL}} - \pi b \int_0^c |'\sigma_{zz}|\Big|_{z=z_0} r dr, \tag{4}$$

where ${}^{\infty}E_{\mathrm{CPDL}}$ is the self-energy of the CPDL in an infinite elastic medium, b is the Burgers vector magnitude of the CPDL, c is the loop radius, $'\sigma_{zz}$ is an additional stress of the CPDL, which is caused by a sphere free surface, z and r are coordinates in the cylindrical coordinate system with the origin at the sphere center (see Fig. 1), and z_0 is the distance from the CPDL plane to the sphere center. The first term in Eq. (4) is well known [29,30]:

$$E^{\infty}_{\mathrm{CPDL}} = \frac{Gb^2 c}{2(1-\nu)}\left(\ln\frac{8c}{r_c} - 2\right) = \frac{Gb^2 c}{2(1-\nu)} \ln\frac{1.08\alpha c}{b}, \tag{5}$$

where r_c is the dislocation core radius, α is a parameter that accounts for the core energy contribution and varies from 0.5 to 5 depending on the material type [31]. The second term in Eq. (4) contains the extra stress $'\sigma_{zz}$ [26]:

$$'\sigma_{zz} = '\sigma_{RR}\cos^2\theta + '\sigma_{\theta\theta}\sin^2\theta - '\sigma_{R\theta}\sin 2\theta, \tag{6}$$

$$'\sigma_{RR} = -2G\sum_{k=0}^{\infty}[A_k(k+1)(k^2-k-2-2\nu)R^k + B_k k(k-1)R^{k-2}]P_k(\cos\theta),$$

$$'\sigma_{\theta\theta} = -2G\sum_{k=0}^{\infty}\Big\{-[A_k(k+1)(k^2+4k+2+2\nu)R^k + B_k k^2 R^{k-2}] \times P_k(\cos\theta) - [A'_k(k+5-4\nu)R^k + B'_k R^{k-2}] \times \frac{dP_k(\cos\theta)}{d\theta}\cot\theta\Big\},$$

$$'\sigma_{R\theta} = -2G\sum_{k=1}^{\infty}[A'_k(k^2+2k-1+2\nu)R^k + B'_k(k-1)R^{k-2}]\frac{dP_k(\cos\theta)}{d\theta},$$

where

$$A_0 = \frac{-b\sin^2\theta_0 R_0^2}{12(1-\nu)a^3}, \quad A_1 = \frac{3D_1}{2(1+\nu)a^5}, \quad A_k = \frac{(2+k)[D_k + 2D_k k + a^2 C_k(1-2k)k]}{2(1+k+k^2+\nu+2k\nu)a^{2k+3}},$$

$$B_0 = 0, \quad B_1 = 0,$$

$$B_k = \frac{-D_k(k^2-1)(k+2)(2k+3) + a^2 C_k(2k+1)[4+(k^2-1)k(k+2)-4\nu^2]}{2(k-1)(1+k+k^2+\nu+2k\nu)a^{2k+1}},$$

$$C_0 = 0, \quad C_1 = 0, \quad C_k = \frac{-b\sin\theta_0 R_0^k}{4(1-\nu)k(2k-1)} P_{k-1}^1(\cos\theta_0), \quad k = 2,3,\ldots;$$

$$D_k = \frac{b\sin\theta_0 R_0^{k+2}}{4(1-\nu)(k+1)(k+2)}\left[-\frac{1-2\nu-(k+1)(k+3)}{2k+3} \times P_{k+1}^1(\cos\theta_0) - (k+2)\cos\theta_0 P_k^1(\cos\theta_0)\right], \quad k = 0,1,2,\ldots;$$

$P_k(t)$ are Legendre polynomials, $P_k^1(t)$ are associated Legendre polynomials, $t = \cos\theta$ or $t = \cos\theta_0$; $R_0 = \sqrt{c^2+z_0^2}$ and $\theta_0 = \arccos(z_0/R_0)$ determine the spherical coordinates of the CPDL line. Performing integration in Eq. (4), one should take into account that $r = z_0\tan\theta$ and $R = z_0/\cos\theta$ at $\theta_0 \neq \pi/2$, and $r = R$ and $\theta = \pi/2$ at $\theta_0 = \pi/2$. The energy E_{CPDL} was analyzed in detail in Ref. [26].

The interaction energy E_{int} is calculated as the work done to generate the vacancy type CPDL in the aforementioned stress field $\sigma_{zz} = \sigma_{RR}\cos^2\theta + \sigma_{\theta\theta}\sin^2\theta$ of distributed stereo disclination, see Eq. (1), and is given by

$$E_{\mathrm{int}} = 2\pi b\int_0^c \sigma_{zz}|_{z=z_0} r dr = 2\pi A\chi\, bc^2\, \ln\frac{R_0}{a} = 2\pi\frac{G(1+\nu)}{3(1-\nu)}\chi\, bc^2\, \ln\frac{c^2+z_0^2}{a^2}. \quad (7)$$

Since $R_0 < a$, this energy is negative for any c and z_0, thus providing the driving force for CPDL generation in the ISP.

The energetic criterion for the CPDL generation inside ISPs is $\Delta E \leqslant 0$ with $\Delta E = 0$ giving the critical condition for the event. With formulas (4), (6) and (7), this equation reads

$$\Delta E = \frac{Gb^2 c}{2(1-\nu)}\ln\frac{c}{\alpha b} - \pi b\int_0^c |'\sigma_{zz}|\Big|_{z=z_0} \mathrm{rdr} + 2\pi\frac{G(1+\nu)}{3(1-\nu)}\chi\, \mathrm{bc}^2\, \ln\frac{c^2+z_0^2}{a^2} = 0. \quad (8)$$

Consider the dependence of the energy change ΔE on the radius c and the position z_0 of the CPDL. It is convenient to use the maps $\Delta E(c/a, z_0/a)$ constructed numerically for fixed values of other parameters of the model. For example, Figure 2a shows such a map built for $a = 100b$, $\nu = 0.3$ and $\alpha = e$, where $e \approx 2.718\ldots$ is the base of the natural logarithm. We take such a value for core-parameter α as an average estimate between 1, typical for metals, and 4, typical for semiconductors, see Ref. [31]. It is seen from the map (Fig. 2a), that the CPDL generation is energetically favorable in the equatorial section of the ISP (at $z_0 = 0$), where the CPDL can nucleate practically in a barrier-less manner and get its optimal radius $c_{\mathrm{opt}} \approx 0.48a = 48b$ at which the energy change reaches the minimum: $\Delta E_{\min} = \Delta E(c = c_{\mathrm{opt}}, z_0 = 0) \approx -0.8Gb^2 a$, see also Figure 2b, which demonstrates the plots $\Delta E(c/a, z_0 = 0)$, the curve corresponding to $a/b = 100$. In other cross-sections of the ISP, i.e. at $z_0 > 0$, the CPDL either must overcome an energy barrier to nucleate at $z_0 < z_0'$, $z_0' \approx 0.425a$, and this barrier increases with z_0, or cannot nucleate at all at $z_0 > z_0'$ because the condition $\Delta E \leqslant 0$ is not fulfilled.

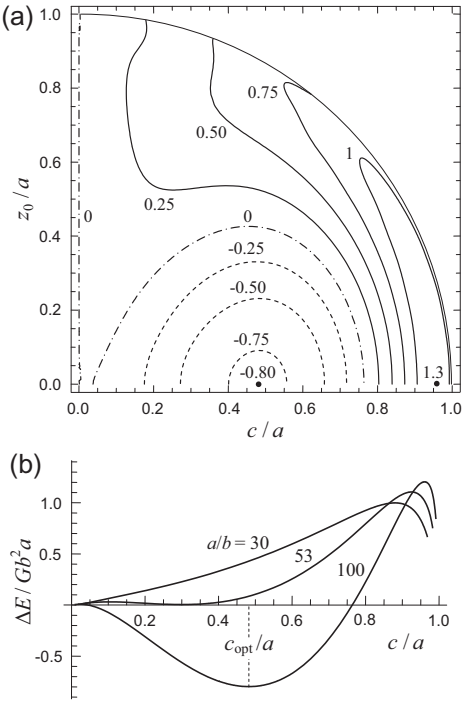

Figure 2. Dependence of the energy change ΔE on the normalized radius c/a and position z_0/a of the CPDL in an ISP of radius a for the dislocation core parameter $\alpha = e$. (a) The map $\Delta E(c/a,\ z_0/a)$ for $a = 100b$, with energy values given in units of Gb^2a. (b) The plot $\Delta E(c/a)$ for $z_0 = 0$ and $a/b = 30$, 53 and 100.

Variation of parameters a and α changes the map $\Delta E(c/a, z_0/a)$. In particular, a decrease in the ISP radius a leads to a decrease of the map region where $\Delta E < 0$ (see Fig. 2a); when a becomes smaller than its critical value $a_{\mathrm{cr}} \approx 53b$, this region disappears, see the curves corresponding to $a/b = 30$ and 53 in Figure 2b. This means that the CPDL cannot nucleate in such a small ISP. When

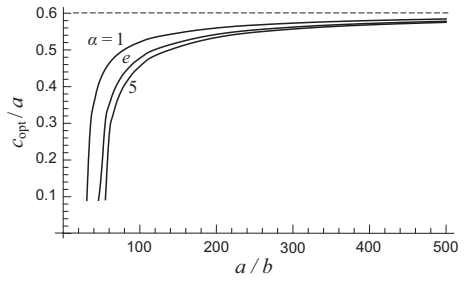

Figure 3. Dependence of the normalized optimal radius c_{opt}/a of the CPDL on the normalized radius a/b of the ISP for the core parameter $\alpha = 1$, e, and 5.

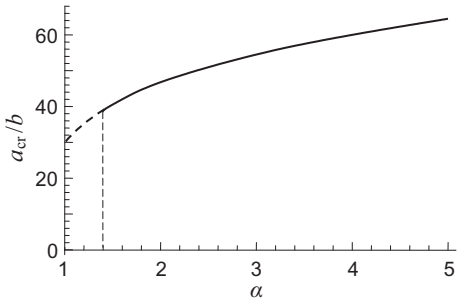

Figure 4. Dependence of the normalized critical radius of the ISP on the core parameter α. The solid and dashed parts of the curve illustrate the $a_{cr}(\alpha)$ and $a'_{cr}(\alpha)$ dependencies, respectively.

$a > a_{cr}$, the CPDL nucleation is energetically favorable, and the normalized optimal radius c_{opt}/a increases with a (see Fig. 3). This increase is rather fast for relatively small values of a, however, it gradually saturates for larger a values, tending to 0.6 in the limit $a \to \infty$.

The effect of the core parameter α on c_{opt}/a is rather strong at relatively small values of a and gradually weakens with increasing a (Fig. 3). The larger is α, the smaller is c_{opt}/a. In contrast, the critical ISP radius a_{cr} noticeably increases with α (Fig. 4). It is interesting that this is true for $\alpha > 1.4$. If $\alpha < 1.4$ (the case of metallic ISPs [31]), the critical ISP radius a_{cr} does not formally exist because $\Delta E < 0$ for small values of c ($> 2b$) at any value of a. On the other hand, however, the optimal CPDL radius c_{opt} must be at least larger than $2b$, and the ISP radius a must be large enough to accommodate such a CPDL: $a > a'_{cr}$. The corresponding part of the curve $a_{cr}(\alpha)$, $1 < \alpha < 1.4$, is shown by the dashed line in Figure 4.

Thus, CPDLs can nucleate in very small ISPs. For example, for $\alpha = 1$, $b = 0.3$ nm and $a \approx a'_{cr} \approx 30b = 9$ nm, the optimal CPDL radius is estimated as $c_{opt} \approx 0.1a \approx 0.9$ nm (Fig. 3). At the same time, the finest ISPs of radius $a < a'_{cr}(\alpha)$ must be free of CPDLs because such ISPs cannot accommodate them.

In summary, we suggested a theoretical model that describes the stress relaxation in ISPs through generation of CPDLs. The distributed stereo disclination continuum model for the initial stress in the ISPs was used. We examined the energy change of the model system and showed that the CPDL nucleation is energetically favorable if the ISP radius a is larger than a critical value a_{cr}, which depends on the dislocation core parameter α. When $a > a_{cr}$, the CPDL nucleates practically in a barrier-less manner in the equatorial section of the ISP and extends until the optimal radius c_{opt}. The normalized optimal radius c_{opt}/a increases with a and tends to 0.6 when $a \to \infty$. An increase in α leads to increase in a_{cr} and decrease in c_{opt}. The smaller ISPs are significantly more sensitive to the α-effect than the larger ISPs. In the special case, when $\alpha < 1.4$, the critical ISP radius is determined by the capability of a fine ISP to accommodate the smallest CPDLs. The finest metallic ISPs with a radius of some nanometers are expected to be free of CPDLs.

This work was supported by the Russian Science Foundation (Grant RSF No. 14-29-00086). A.L.K., L.M.D., A.A.V. and A.E.R. were also supported, in part, by a grant from the Ministry of Education and Science of the Russian Federation (Decree No. 220) obtained by the Togliatti State University under the contract No. 14.B25.31.0011.

[1] H. Hofmeister, Cryst. Res. Technol. 33 (1998) 3.
[2] M.J. Yacaman, J.A. Ascencio, H.B. Liu, J. Gardea-Torresday, J. Vac. Sci. Technol. B 19 (2001) 1091.
[3] K. Koga, K. Sugawara, Surf. Sci. 529 (2003) 23.
[4] I.S. Yasnikov, Tech. Phys. Lett. 34 (2008) 944.
[5] D. Seo, C.I. Yoo, I.S. Chung, S.M. Park, S. Ryu, S. Hyunjoon, J. Phys. Chem. C 112 (2008) 2469.
[6] A.E. Romanov, A.A. Vikarchuk, A.L. Kolesnikova, L.M. Dorogin, I. Kink, E.C. Aifantis, J. Mater. Res. 27 (2012) 545.
[7] R. De Wit, J. Phys. C Solid State Phys. 5 (1972) 529.
[8] A. Howie, L.D. Marks, Philos. Mag. A 49 (1984) 95.
[9] V.G. Gryaznov, J. Heidenreich, A.M. Kaprelov, S.A. Nepijko, A.E. Romanov, J. Urban, Cryst. Res. Technol. 34 (1999) 1091.
[10] A.S. Barnard, J. Phys. Chem. B 110 (2006) 24498.
[11] R. Könenkamp, R.C. Word, M. Dosmailov, A. Nadarajah, Phys. Status Solidi (RRL) 1 (2007) 101.
[12] V.G. Gryaznov, A.M. Kaprelov, A.E. Romanov, I.A. Polonskii, Phys. Status Solidi B 167 (1991) 441.
[13] A.E. Romanov, I.A. Polonsky, V.G. Gryaznov, S.A. Nepijko, T. Junghanns, N.I. Vitrykhovski, J. Cryst. Growth 129 (1993) 691.
[14] Y.T. Pei, J.Th.M. de Hosson, Acta Mater. 49 (2001) 561.
[15] A.L. Kolesnikova, A.E. Romanov, Phys. Status Solidi (RRL) 1 (2007) 271.
[16] I.S. Yasnikov, A.A. Vikarchuk, Tech. Phys. Lett. 33 (2007) 817.
[17] X. Fu, J. Jiang, W. Zhang, J. Yuan, Appl. Phys. Lett. 93 (2008) 043101.
[18] C. Langlois, D. Alloyeau, Y. LeBouar, A. Loiseau, T. Oikawa, C. Mottetd, C. Ricolleaua, Faraday Discuss. 138 (2008) 375.
[19] L.M. Dorogin, S. Vlassov, A.L. Kolesnikova, I. Kink, R. Lõhmus, A.E. Romanov, Phys. Status Solidi B 247 (2010) 288.
[20] M.Yu. Gutkin, S.N. Panpurin, J. Macromol. Sci. B Phys. 52 (2013) 1756.
[21] I.S. Yasnikov, JETP Lett. 97 (2013) 513.
[22] M.Yu. Gutkin, S.N. Panpurin, Phys. Solid State 56 (2014) 1187.
[23] A.E. Romanov, L.M. Dorogin, A.L. Kolesnikova, I. Kink, I.S. Yasnikov, A.A. Vikarchuk, Tech. Phys. Lett. 40 (2014) 174.
[24] I.S. Yasnikov, Tech. Phys. Lett. 40 (2014) 411.
[25] A.L. Kolesnikova, A.E. Romanov, Tech. Phys. Lett. 33 (2007) 886.
[26] A.L. Kolesnikova, M.Yu. Gutkin, S.A. Krasnitckii, A.E. Romanov, Int. J. Solids Struct. 50 (2013) 1839.
[27] M.Yu. Gutkin, A.L. Kolesnikova, S.A. Krasnitckii, A.E. Romanov, Phys. Solid State 56 (2014) 723.
[28] M.Yu. Gutkin, A.L. Kolesnikova, S.A. Krasnitckii, A.E. Romanov, A.G. Shalkovskii, Scr. Mater. 83 (2014) 1.
[29] J. Dundurs, N.J. Salamon, Phys. Status Solidi B 50 (1972) 125.
[30] A.L. Kolesnikova, A.E. Romanov, Preprint No. 1019, Ioffe Physico-Technical Institute, Leningrad, 1986 (in Russian).
[31] J.P. Hirth, J. Lothe, Theory of Dislocations, second ed., Wiley, 1982.